PHYSICAL REVIEW D **84,** 042002 (2011)

Muon excess at sea level from solar flares in association with the Fermi GBM spacecraft detector

C. R. A. Augusto, C. E. Navia, H. Shigueoka, and K. H. Tsui
Instituto de Física, Universidade Federal Fluminense, 24210-346, Niterói, Rio de Janeiro, Brazil

A. C. Fauth
Instituto de Física Gleb Wathagin, Universidade Estadual de Campinas, Campinas, São Paulo, Brazil
(Received 1 March 2011; revised manuscript received 28 June 2011; published 26 August 2011)

This paper presents results of an ongoing survey on the association between muon excesses at ground level, registered by the Tupi telescopes, and transient solar events, whose gamma-ray and x-ray emissions were reported by the Fermi Gamma Burst Monitor and the Geostationary Operational Environmental Satellite 14, respectively. We show that solar flares of small scale, those with prompt x-ray emission classified by the Geostationary Operational Environmental Satellite as C-Class with power 10^{-6} to 10^{-5} Watts m^{-2} at 1 AU, may give rise to muon excess probably associated with solar protons and ions emitted by the flare and arriving at the Earth as a coherent particle pulse. The Tupi telescopes are within the central region of the South Atlantic Anomaly, where the geomagnetic field intensity is the lowest on the Earth. Here we argue for the possibility of a ''scale-free'' power-law energy spectrum of particles accelerated by solar flares. For energies around and exceeding the pion production, large and small scale flares have the same power-law energy spectrum. The difference is only in the intensity. The Tupi events give support to this conjecture.

DOI: 10.1103/PhysRevD.84.042002 PACS numbers: 96.60.qe, 95.55.Ev, 95.55.Vj, 96.50.Vg

I. INTRODUCTION

The last solar cycle 24 started at the beginning of 2008 [1]. Nevertheless, in the second half of 2010, we were still at a low level of activity, in an anomalously extended period of solar minimum. This solar cycle anomaly is the first in the space era, where the Sun is monitored by spacecraft detectors. But there was a similar pattern registered 107 yr ago during the transition between cycles 13 and 14. Solar flares are among the most powerful astrophysical phenomena in the solar system. At the beginning, the observation and the study of these solar flares used detectors on the surface of the Earth, mainly by neutron monitor experiments [2–4]. A lot has been obtained with these observations, such as the anticorrelation between solar activity and the flow of galactic cosmic rays; the existence of a prompt and late emission in flares; their correlations with coronal mass ejection and Forbuch event, which is a fall in the cosmic ray intensity due to a solar disturbance crossing the Earth; and so forth.

However, in most cases, the observations are restricted for flares with high intensities. Those with an x-ray flux at 1 AU above 10^{-4} Watts m^{-2} is classified by Geostationary Operational Environmental Satellite (GOES) as X-Class flares, and above 10^{-5} Watts m^{-2} as M-Class flares. Recently the Tupi experiment has reported experimental evidence of muon excess in association with high energy particles (protons and ions) with energies above the pion production threshold (because they produce muons in the atmosphere), emitted by flares of small scale, those with an x-ray flux below 10^{-5} Watts m^{-2} or C-Class flares [5,6].

Even in events observed at ground level in association with large solar flares, the acceleration mechanism producing particles (protons and ions) up to several tens of GeV is not well understood. The situation becomes still more critical in the case of ground events associated with solar flares of small scale. Here we argue for the possibility of a scale-free energy distribution of particles accelerated by solar flares. This means that high and low fluxes of solar particles, associated to big and small flares, have the same energy spectrum, up to energies exceeding the pion production. The difference between them is only the intensity. This hypothesis is corroborated by new observations of two solar flares of small scale, observed by the Tupi telescopes in association with energetic gamma-rays detected by Fermi Gamma Burst Monitor (GBM) (designed to observe gamma-ray bursts) and with x-ray flux detected by GOES 14–both are spacecraft detectors orbiting the Earth.

This paper is organized as follows: In Sec. II, a brief description of the Tupi experiment is presented. In Sec. III, we argue why the telescopes have a high sensitivity. Section IV gives a brief description of micro and mini solar flares. A brief study on muon excess and solar flare association is presented in Sec. V. Section VI is devoted to show the results of the association between muon excesses at ground level and two solar mini flares, registered by GOES 14 (x-ray flux) and Fermi GBM (gamma-ray counting rate). Section VII contains an analysis of the pitch angle, and Sec. VIII is devoted to a spectral analysis, where the ''heart'' of the calculations is the Monte Carlo results for the proton muon conversion in the Earth's atmosphere. Section IX contains conclusions and remarks.

II. THE TUPI EXPERIMENT

The Tupi experiment [7] is an Earth-based muon apparatus, devoted to the study of cosmic rays, located in Niteroi City, Rio de Janeiro, Brazil (22.88 S, 43.16 W), consequently near the SAA central region. The apparatus has two telescopes. Each telescope was constructed on the basis of two detectors of plastic scintillators, 0.5 m $\times$ 0.5 m $\times$ 35 mm, placed perpendicularly to the axis of the telescope. The distance between the plastic scintillators is 3 m. The general layout of the vertical telescope, including the data acquisition, is shown in Fig. 1. The data acquisition system is made on the basis of a Universal Serial Bus card, with a counting rate of up to 100 kHz per channel. All steps from signal discrimination to the coincidence and anticoincidence are made via software, using the virtual instrument technique. The application programs were written using the LAB-VIEW tools. The Tupi experiment has a fully independent power supply, with an autonomy of up to 6 h to safeguard against local power failures. As a result, the data acquisition is carried out 24 h a day, giving a duty cycle greater than 90%.

The main task of the first level trigger is a coincidence between the two detectors. The second level trigger is a veto for air shower coming from other directions and contains a third detector placed off the telescope axis. Thus the directionality of each muon telescope is guaranteed by a veto or anticoincidence guard, using a third detector. Therefore, only muons with trajectories close to the telescope axis are registered. One of the two telescopes has a vertical orientation, and the other is oriented near 45° to the vertical (zenith) pointing to the west. Both telescopes have an effective aperture of 65.6 cm^2 sr, projecting to the space a cone with an opening angle of 9.5° with respect to the telescope axis.

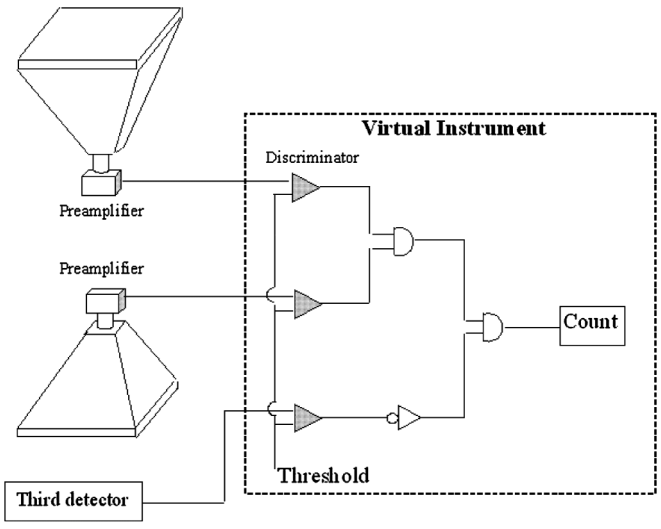

FIG. 1. General layout of the vertical telescope including the logic implemented in the data acquisition system using LAB-VIEW software.

III. LOCATION OF THE TUPI TELESCOPES

The Earth is surrounded by the magnetosphere which protects us from cosmic rays with energies less than several GeV by deflecting or capturing them in the Van Allen radiation belts. Nevertheless, there is an additional factor that may locally enhance the cosmic ray intensity at middle latitudes. This is the so-called South Atlantic Anomaly, which is an area of anomalously weak geomagnetic field strength. In the International Geomagnetic Reference Field 95 data [8], the magnetic field strength in the central SAA region (26 S, 53 W) is 22 000 nano Tesla (nT), and the Stormer rigidity cutoff is around 7 GV. This area coincides with the Atlantic coast to the southwest of Brazil, while the total SAA area covers a great part of South America's central region. The boundary region is defined as where the magnetic field strength is less than 30 000 nT, as shown in Fig. 2.

The SAA is a result of the eccentric displacement of the magnetic field center from the geographical center of the Earth (by about 400 km) as well as the displacement between the magnetic and geographic poles of the Earth. This behavior permits the inner Van Allen belt to impart highly energetic particles (mostly protons), penetrating deeper into the atmosphere owing to the low field intensity over the SAA, and thereby interacting with the dense lower atmosphere, resulting in higher ionization and increased electrical conductivity [9].

It has been shown that the SAA region [10] also favors the precipitation of high energy particles (Van Allen background), mostly in the MeV energy range, going up to energies above the pion production threshold, because they produce air showers in the Earth's atmosphere and the hard component (muons) is able to reach sea level [10].

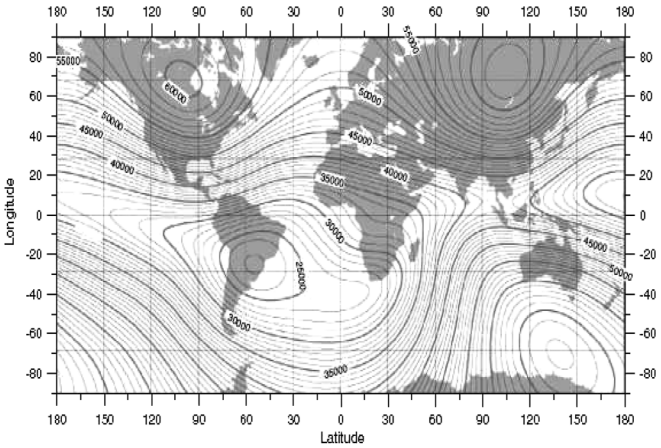

FIG. 2. Geographic distribution of geomagnetic field intensity, according to USA/UK Magnetic chart Epoch 2000. The unit is in nano Tesla (nT), and the contour interval is 2000 nT. The SAA boundary is around $B = 30\,000$ nT. The Tupi telescopes location is close to SAA central region, where the magnetic field is around 23 000 nT.

The Van Allen background has an enhancement at daytime, beginning 3 h after sunrise until around 1 h after sunset. During this interval, the focusing effect of the interplanetary magnetic field (IMF) lines become dominant, and they point to the Earth's surface.

On the other hand, in the Earth's upper atmosphere, there is the ionosphere (100 km above sea level) which is characterized by a larger ion concentration [11]. However, in the stratosphere at low and middle latitudes, starting from 12 km above sea level, there is a residual ion concentration [12]. The ionization in this region is mainly due to cosmic rays, and the effect is an increase in the electric conductivity of the stratosphere. In the SAA region this effect is enhanced due to the Van Allen background, especially in the daytime. A consequence of this behavior is an increase in the range of charged particles. For instance, in the SAA region, cosmic ray fluxes are even higher than world averages at comparable altitudes, reflecting an enhancement of incoming primary cosmic rays.

IV. SOLAR FLARES OF SMALL SCALE

A solar flare is defined as a sudden, rapid, and intense variation in brightness. A solar flare occurs when magnetic energy that has built up in the solar atmosphere is suddenly released. Radiation is emitted across virtually the entire electromagnetic spectrum. In solar flares, the interaction of the energetic electrons with thermal protons provides the deceleration, and x-ray photons with energies less than or nearly equal to the electron energy are produced. These x-ray photons are the emitted radiation signatures detected by scientific instruments such as GOES and Solar and Heliospheric Observatory. The frequency of flares coincides with the 11-yr solar cycle. When the solar cycle is at a minimum, active regions are small and rare and few solar flares are detected. Their occurrence increases in number as the Sun approaches the maximum of its cycle. However, the period around the solar minimum is useful for the observation of small transient events, such as micro and mini flares, whose flux is less than 10^{-5} Watts m^{-2}.

Harder x rays with energies greater than 10 keV are also believed to be electron-ion bremsstrahlung. Spectral measurements of such hard x rays follow a power law rather than an exponential shape. However, the gamma radiation observed in a solar flare has several origins. The bremsstrahlung spectrum can extend up to the gamma-ray range. Indeed, in some of the biggest flares, the spectrum is seen to extend to energies in excess of 100 MeV. Proton and heavy ion interactions also produce gamma-rays through π^0 decay, resulting in a spectrum that has a maximum at 68 MeV. A continuous spectrum and many individual gamma-ray lines have been identified, and they result from decay of excited elements in the solar atmosphere as carbon, nitrogen, etc., that are excited to high energy states in various nuclear interactions.

V. ASSOCIATION BETWEEN MUON EXCESS AND SOLAR FLARE

The association between an x-ray flare and a muon excess has to take into account the delay between the flare start and the time of flight from the Sun to the Earth of energetic solar particles along solar magnetic field lines, the so-called ''garden hose'' line schematized in Fig. 3. Flares located near the footpoint of the garden hose field line between the Sun and Earth (good connection) reach the Earth with a pitch angle close to 45°. The time of flight is estimated from simulations under the assumption that energetic particles, released by a flare-driven shock, are injected into the interplanetary medium in coherent pulses which propagate along realistic Archimedean spiral field lines around the Sun [13]. Here, we summarize simulation results for a typical arc length along the magnetic field line, $\langle z \rangle = 1.3$ AU, as a function of the distance traveled, S, which can be expressed as

$$\langle z \rangle = \alpha(\lambda) S. \tag{1}$$

The constant $\alpha(\lambda)$ depends on the scattering mean free path λ, and satisfies the constraint condition $\alpha(\lambda) = 1$ at $\lambda = 1$ AU. This condition is sometimes called the scatter-free condition, which implies that particles freely stream along the field line at their maximum speed like a coherent particle pulse. In other words, the focus effect of the IMF lines becomes dominant and the propagation of energetic particles is like coherent pulses, following trajectories along the IMF lines. On the other extreme, when the scattering mean free path is small compared to the scale length of the IMF (i.e., $\lambda \leq 0.2$ AU), particle propagation follows

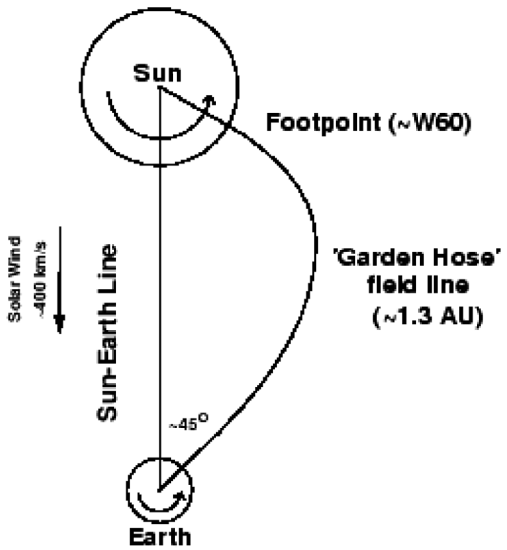

FIG. 3. Magnetic field connection between the Sun and Earth. Flare particles (protons) injected into the space travel close to the direction of the garden hose field lines between the Sun and Earth. They arrive at the Earth with an angle close to 45°, relative to the sunward direction, which defines the magnetic sunward direction, from Dulding [19].

helical trajectories along the IMF lines. Fluctuations of small scales in the IMF act as scattering centers of the particles and the propagation is dominantly diffusive.

A muon excess detected at sea level by a directional telescope is the signature of primary particles arriving at the top of the atmosphere with a strong anisotropic pitch angle distribution as an ''almost coherent pulse''. The rise time in the time profile of the muon excess can be used to infer the coherence of a pulse. For instance, a very short rise time suggests a nondiffusive coherent particle pulse transport. Thus an almost coherent pulse has $\lambda \geq 0.2$ AU and corresponds to a time of flight of energetic particles with a mean rigidity of 1 GV of up to 35 min. This delay corresponds to up to $\sim$27 min relative to the x-ray signal at 1 AU. Solar flare detection at ground level depends on several aspects, such as a good magnetic connection between the Sun and Earth. Most solar flares associated with ground level events are located on the western sector of the Sun where the IMF is well connected to the Earth.

VI. RESULTS

The GOES 14 Ion Chamber Detectors provide whole-Sun x-ray fluxes for the 0.5–4 and 1–8 $\dot{A}$ wavelength bands. In most cases, the GOES x-ray fluxes of solar flare are used as a reference for other types of detection, such as ground level detectors and the Fermi GBM. In addition, the Fermi GBM detector is designed to observe gamma-ray bursts (GRBs) in the field of view of the GBM instrument, and in the energy range 10 keV to 30 MeV. Hereafter, all the time bins of the Tupi data are tested with a bin selection criterion. The significance of the signal in the i-th bin is defined as $\sigma_i = (C^{(i)} - B)/\sqrt{B}$, where $C^{(i)}$ is the measured number of counts in the i-th bin, and B is the averaged number of background counts.

A. The event on 4 October 2010

The muon enhancement on 4 October 2010 is a peak in the muon counting rate ($E_\mu > 0.1$ GeV) observed in the vertical muon telescope. The onset in time correlation has large statistical significance (7.1σ) when the counting rate is 5 min binning. The muon arrival excess is 12.4 min later relative to the arrival of an x-ray excess flux on GOES 14. This means that the time of flight from the Sun to the Earth of the energetic particles was 20 min. According to the criteria established in Sec. V, the muon excess was formed by primary particles arriving at the top of the atmosphere as an almost coherent pulse, and with a rigidity above 1 GV (1 GeV for protons). This is a mini flare whose x-ray prompt emission is classified as C2-class (a flux of 1.9×10^{-6} Watt/cm^2). Figure 4 shows the GOES 14 x-ray prompt emission on 4 October 2010 for two wavelengths in the top panel, and the corresponding (vertical) Tupi muon counting rate (5 min binning) in the bottom panel. There is no signal in the inclined telescope.

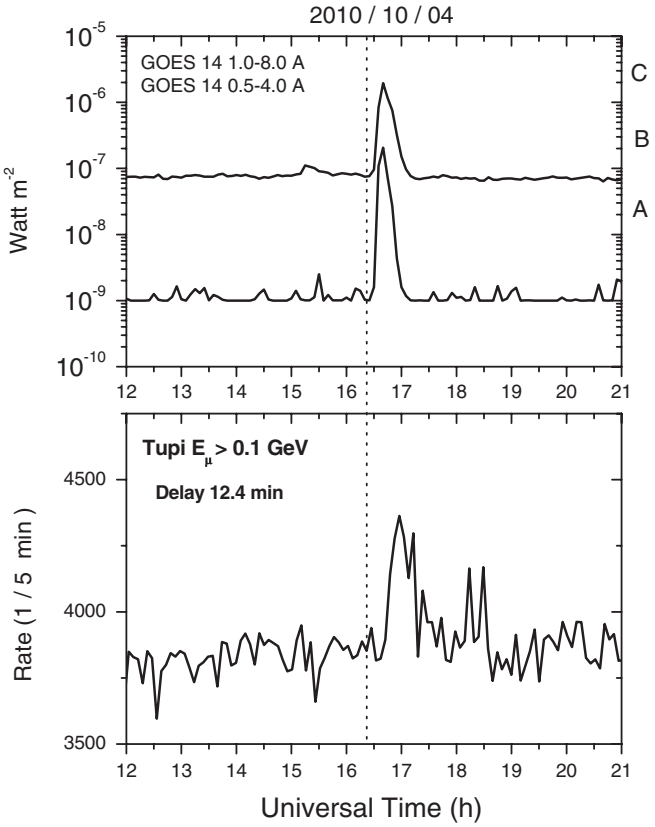

FIG. 4. Top panel: The x-ray flux on 4 October 2010, according to GOES 14, for two wavelengths. Bottom panel: The 5-min muon counting rate in the vertical Tupi telescope.

On the other hand, solar flare events have been searched since 2008 by the Fermi GBM. So far, even in the last solar minimum period, the Fermi GBM has found evidence of a high energy photon emissions (gamma-rays) from solar flares. From 27 October 2009 to 3 November 2010, 22 solar flares have been registered by the Fermi GBM. Solar activity is expected to rise in the coming months, reaching a maximum in 2012, and the number of flares observed by the GBM must increment by a factor of up to ten for the same period. For the first flare here analyzed and observed on 4 October 2010, the Fermi GBM trigger was at 16:32:31.443 UT, and it was classified as a solar flare with a reliability of 0.8. The Fermi gamma counting rate is shown in Fig. 5 (top panel). It has a very fast rise time, even faster than the emission of x-rays observed by GOES 14 (see Fig. 4, top panel). In contrast, the rise time observed in the time profiles of the muon counting rate is not so fast as is shown in Fig. 5 (bottom panel). This shows a certain degree of diffusion of the particle energy emitted by the flare during its transport. The beginning of the muon excess is 4.5 min later relative to the Fermi GBM trigger. However, the flare duration (gamma-ray emission) in the Fermi GBM is short compared to the x-ray emission and the muon excess time widths. The gamma-ray emission as observed by Fermi does not exceed 467 sec (a narrow

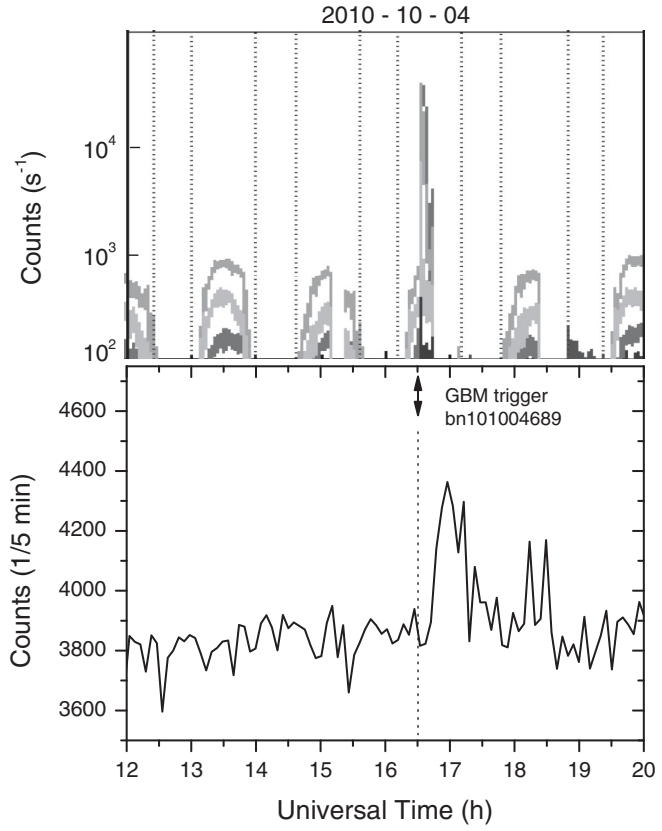

FIG. 5. Top panel: Fermi GBM gamma-ray counting rate on 4 October 2010, in the energy band of 6–300 keV expressed by the gray scale (the darkest corresponds the more energetics). The flare gamma signal starts at 16:32:31.443 UT (Trigger bn101004689). Bottom panel: The 5-min muon ($E_\mu >$ 100 MeV) counting rate in the vertical Tupi telescope.

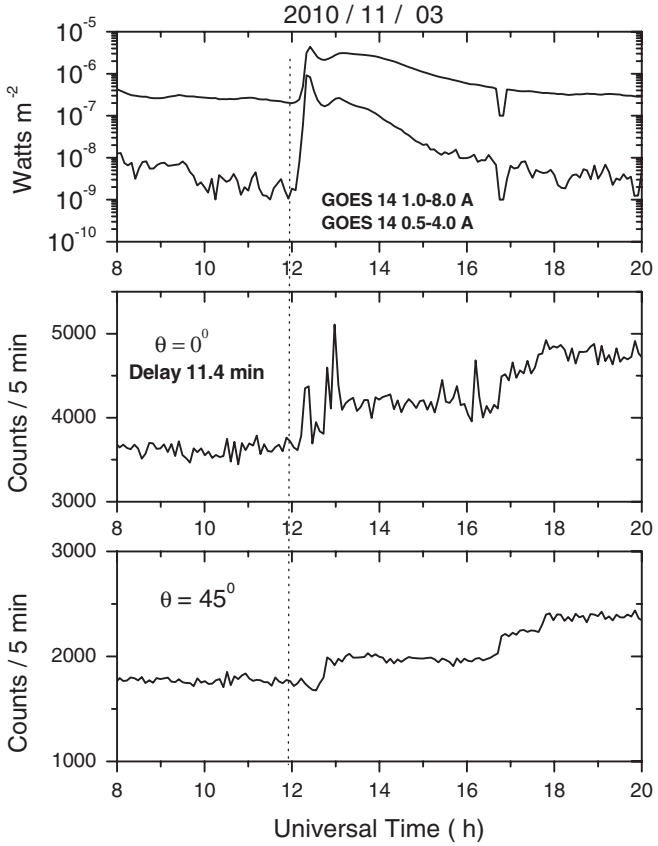

FIG. 6. The same as Fig. 4. There is a flare signal on 3 November 2010, which appears only in the vertical Tupi telescope.

peak), while the x-ray emission and the muon excess have durations over 2000 sec.

B. The event on 3 November 2010

The muon enhancement on 3 November 2010 has two sharp peaks in the muon counting rate observed in the vertical muon telescope. The onset in time correlation has very high statistical significance of up to 20σ when the counting rate is 5 min binning. The arrival of the muon excess is 11.4 min later relative to the arrival of an x-ray excess flux at GOES 14, as is shown in Fig. 6 (top panel) together with the muon counterpart (bottom panel). This mean that the muon excess was formed by primary particles arriving at the top of the atmosphere as a coherent pulse, and with a rigidity above 1 GV. We see again that no signal exists in the inclined telescope. This flare is more intense than the previous one, and it is of C5-class. In addition, it is possible to see two serial peaks in both the x-ray flux and muon counting rate time profiles. The time interval between these two serial peaks in both GOES 14 x-ray flux and Tupi muon excess is about 38 min. That is a signature of little diffusion of the particles during their transport from the Sun to the Earth following IMF lines.

For this second flare, the Fermi GBM trigger was at 12:13:10.916 UT, and it was classified as a solar flare with a reliability of 0.92. The Fermi GBM light curve is shown in Fig. 7 (top panel), and in the same figure is shown the time profile (bottom panel7, raw data) of the muon counting rate. In this case, both the muon excess and the GOES 14 x-ray flux have a faster rise time than the rise time observed in the Fermi GBM light curve. The gamma-ray emission duration as observed by Fermi GBM is short (1295 sec) in comparison to the muon excess duration of around 1 h. This is in contrast to the long duration of the x-ray emission as observed by GOES 14, because after a fast rise time it falls off slowly. However the two peaks observed in the muon counting rate during the first 500 sec, as shown in Fig. 7, are in excellent correlation with the two peaks observed in the Fermi GBM. In addition, the time delay of the muon excess relative to the gamma-ray detection by Fermi (at 1 AU) is less than 33 sec. Again, this is a signature indicating a nondiffuse transport of the charged particles emitted by the solar flare.

We can see that there is also a delay between GOES and Fermi in both events. As explained in Sec. IV, x rays and

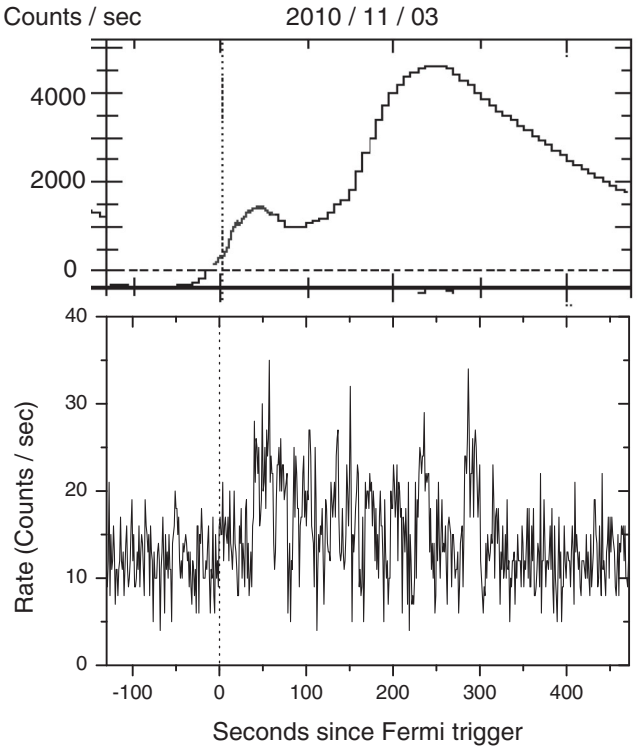

FIG. 7. Comparison between the Fermi GBM light curve for the flare on 3 November 2010 (top panel) and the muon time profiles observed by the Tupi vertical telescope (bottom panel). In both cases, the data is 1-sec binning.

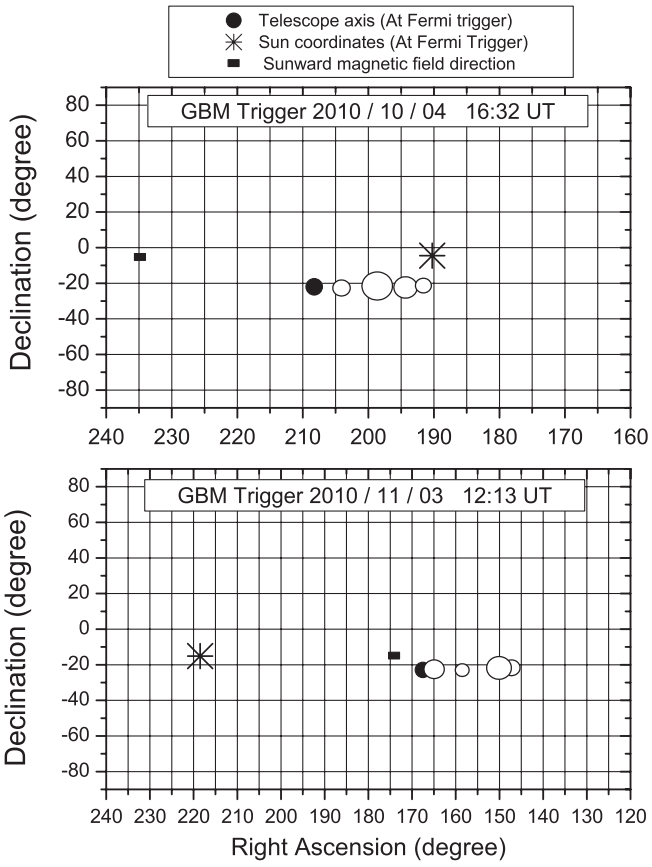

FIG. 8. Sun location (asterisk), at Fermi trigger time and the vertical telescope axis location during the sky scanner due to the Earth rotation, for the case of the two flares here analyzed. The diameter of the open circles is proportional to the logarithm of the muon counting rate. The angular separation between the sunward (asterisk) and magnetic sunward (rectangle) directions has a nominal 45°. The pitch angle is the angle between the sunward magnetic direction and the telescope axis direction (direction of propagation of muons). The pitch angles are 27° for the first event and 6° for the second one.

gamma-rays have different origins. X rays are produced by electron bresstrahlung process and gamma-rays are produced by nuclear process. It is possible to observe a minor difference between Fermi and Tupi, because Tupi detects muons in the atmospheric cascade generated by the protons in the terrestre atmosphere. These protons while in the solar atmosphere generate the gamma-rays through nuclear interactions. In the interplanetary space, gamma-rays travel at straight lines at light speed, while protons follow the garden hose magnetic field lines at relativistic speed, which accounts for the different time lags.

VII. PITCH ANGLE ANALYSIS

Figure 8 shows the Sun location (asterisk) at Fermi trigger time, and the muon excess location (black circle) of Tupi telescope, and the evolution time (open circles) during the sky scanner of the vertical telescope due to the Earth's rotation, for the case of the two flares here analyzed. The diameter of the open circles is proportional to the logarithm of the muon counting rate. In both cases, the difference between the Sun and telescope axis declination is small, with $\Delta\delta = 17.2$ and $\Delta\delta = 7.5$, respectively. Thus the angular separation between the sunward direction and the direction of the telescope axis is approximately equal to the difference between the right ascension of the Sun and the axis direction of the telescope. Following Fig. 8, we can observe an angular separation around 18° for the first event and 51° for the second one.

The charged particles emitted by a flare follow the solar magnetic field lines (Parker spiral), which defines the sunward magnetic field direction, represented by squares in Fig. 8. The solar field lines overtake the Earth magnetosphere with a nominal 45° relative to the sunward direction (see Fig. 3). It is possible to define the pitch angle as the angle between the telescope viewing direction (asymptotic cone of acceptance) and the sunward magnetic field direction. A telescope direction with 0° pitch angle views particles coming from the Sun along the sunward magnetic direction. Thus the pitch angle is 27° for the first event, and 6° for the second one.

Because of Earth's rotation the pitch angle has a temporal evolution, and its extension depends on the event duration. For instance, in our case, a solar flare with a

duration of 1 h corresponds to a variation of 15° in the pitch angle. The temporal evolution of the pitch angle for the first event was from 27° to 45°, and in the case of the second event, the evolution of the pitch angle was from 6° to 18.5°.

On the other hand, the rise time in the time profiles of the muon counting rate provides valuable information on the characteristics of the propagation of particles emitted in solar flares. In general, a nondiffusive propagation of solar particles is characterized by a coherent pulse of particles arriving at the top of the atmosphere, giving a fast rise time in the detected signal. This effect is enhanced if the detector has a good magnetic connection with the Sun. That is the detected event will have a small pitch angle, which is the case of the second event. In addition, a more prolonged rise time, as observed in the time profiles of the muon excess of the first event, means a more accentuated diffusion of the particles.

VIII. SPECTRAL ANALYSIS

The minimum proton energy needed to produce muons of energy E_μ in the atmosphere is $E_{\rm pth} \sim 10 \times E_\mu$. In the case of the Tupi experiment, the muon energy threshold is $E_\mu \sim 0.1$ GeV. This means that the minimum proton energy is $E_{\rm pth} \sim 1.0$ GeV. This energy corresponds to a rigidity of 1 GV, and it is below the Stormer geomagnetic rigidity cutoff in the SAA region (~ 7 GV). However, Monte Carlo results [14] have shown at Tupi conditions that an effective proton energy threshold for muon production in the atmosphere is $E_{\rm pth} \sim 10$ GeV as is shown in Fig. 9, where the specific yield function, which is the number of muons at sea level per proton, as a function of proton energy near the vertical direction, is determined according to the FLUktuierende KAskade (FLUKA) Monte Carlos results [15] and Honda *et al.* [14]. This FLUKA result can be described by the following fitting

$$S(E_p > 10\ \text{GeV}) = A_{\mu_1} E_p^{\nu_1} \exp(-(E_{0_1}/E_p)^{\lambda_1}) \quad (2)$$

$$S(E_p < 10\ \text{GeV}) = A_{\mu_2} E_p^{\nu_2} \exp(-(E_{0_2}/E_p)^{\lambda_2}), \quad (3)$$

where $A_{\mu_1} = (7.8 \pm 0.60) \times 10^{-3}$, $A_{\mu_2} = (6.8 \pm 0.50) \times 10^{-3}$, $\nu_1 = 1.18 \pm 0.014$, $\nu_2 = 1.18 \pm 0.014$, $E_{0_1} = 10.2 \pm 0.6$ GeV, $E_{0_2} = 10.2 \pm 0.7$ GeV, $\lambda_1 = 1.48 \pm 0.12$, $\lambda_2 = 1.0 \pm 0.0$

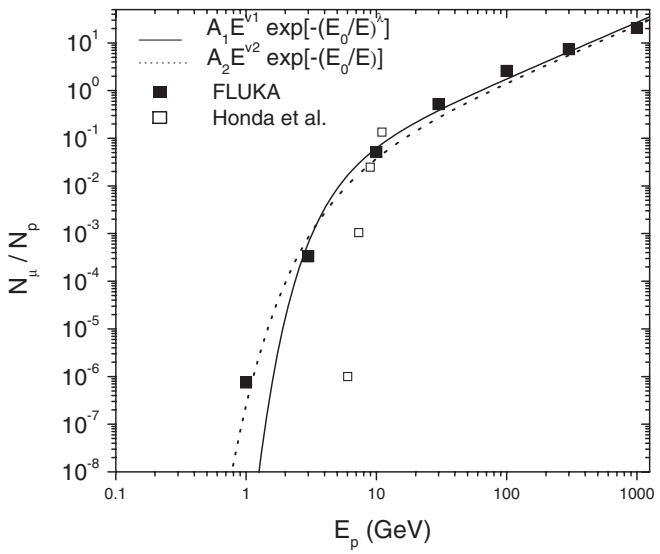

FIG. 9. Yield function, as the number of muons at sea level per proton focusing vertically at the top of the atmosphere, as a function of proton energy. The black squares represent the FLUKA Monte Carlo results [15], the open squares are results from [14] under Tupi conditions and the lines are two parameterizations.

The energy spectra and timing of some of the largest solar particle events of solar cycle 23 have been obtained using data from Advanced Composition Explorer, Solar Anomalous and Magnetospheric Particle Explorer, and GOES [16]. The energy spectra of accelerated protons evolve from soft to hard gradually with time. The origin of this behavior is that the charged particles accelerated by solar flares have a power energy spectrum. However, when the energies exceed the threshold of the production of pions, the almost elastic collisions in the atmosphere of the Sun becomes inelastic, and they lose energy via nuclear interactions (pion production). This transition produces a shift in the spectral index, and the spectrum becomes more steep. Thus, these spectra are all well fit by a double power-law form.

The energy region of our interest, $E_p \geq 10$ GeV, is above the transition region, that is, inside the hard part, with a spectral index ranging from -2 to -5. The spectral index obtained from observations is an integration over time. There is almost no information on how the energetic particle spectrum changes with time, which introduces some uncertainty in the value of the index. We assumed that the energy spectrum of protons ($E_p \geq 10$ GeV) emitted in solar flares (hard part) is fitted by a single power-law function:

$$J(E_p) = A_p \left(\frac{E_p}{\text{GeV}}\right)^{-\beta}. \quad (4)$$

The total number of muons at sea level with energies above E_μ covering an effective area $S_{\rm eff}$, and in an integrated time T, is a convolution between Eq. (2) (or Eq. (3)) and Eq. (4),

$$N_\mu(\geq E_\mu) = S_{\rm eff} T \int_{E_{p_{\rm min}}}^{\infty} S(E_p) J(E_p, T) dE_p, \quad (5)$$

since the muon intensity, given by the integral energy spectrum, is

$$I_\mu(>E_\mu) = \frac{N_\mu(\geq E_\mu)}{S_{\rm eff} T}. \quad (6)$$

The muon excess allows us to obtain the coefficient, A_p, of the primary proton spectrum as

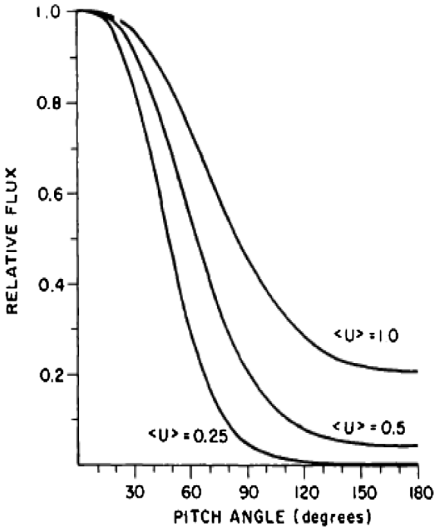

FIG. 10. Expected pitch angle distribution of the anisotropic flare particle flux, observed on Earth's surface during various phases.

$$A_p = I_\mu(>E_\mu)\frac{1}{A_\mu} \times \left(\int_{E_{p\min}}^{\infty} dE_p \left\{\left(\frac{E_p}{\mathrm{GeV}}\right)^{-\beta+\nu} \exp\left[-\left(\frac{E_0}{E_p}\right)^{\lambda}\right]\right\}\right)^{-1}. \quad (7)$$

These results must be corrected in order to take into account the experimental bias. For instance, it is possible to assume that the standard garden hose lines are the probable direction of maximum particle flux. Under this condition, the asymptotic cone of acceptance of the vertical telescope had an associated pitch angle of 27° for the event on 4 October 2010, and a pith angle of 6° for the event on 3 November 2010, both at Fermi GBM trigger time. From the average expected pitch angle distribution [17] of a coherent anisotropic particle flux, as is shown in Fig. 10, it is possible to see, for a pitch angle less than 20°, the particle flux is inside the acceptance cone, and the anisotropic corrections are irrelevant. This is valid for all phases of the pitch angle distribution evolution.

The temporal evolution of the pitch angle for the first event was from 27° to 45° given a reduction of around 10% in the muon flux. In the case of the second event, the evolution of the pitch angle was from 6° to 18.5° given a reduction smaller than 2% in the muon flux. The results

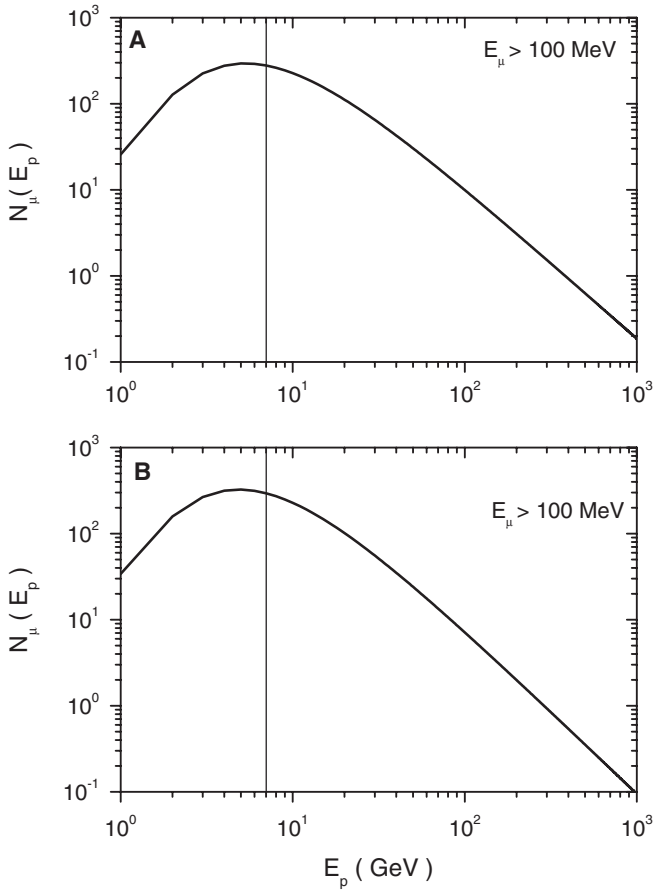

FIG. 11. Number of muons ($E_\mu > 0.1$ GeV) detected in the vertical Tupi telescope, produced by solar flare particles (protons) with energies between E_p and $E_p + dE_p$. (a) for the event on 4 October 2010 and (b) for the event on 3 November 2010. The vertical lines represent the Stormer rigidity cutoff at Tupi telescope's location.

of proton flux at 1 AU coming from solar flares, on the basis of the FLUKA Monte Carlo and the observed muon flux at sea level, are listed in Table I for the two events here analyzed. The shape of the number of muons ($E_\mu > 0.1$ GeV), detected in the vertical Tupi telescope, produced by solar flare particles (protons) with energies between E_p and $E_p + dE_p$, is shown in Fig. 11 for two events here analyzed. The vertical lines represent the vertical Stormer rigidity cutoff at Tupi telescope's location. The main peculiarity of these spectra is their similarity, and

TABLE I. Differential and integral energy spectrum of solar flare particles, obtained from FLUKA simulation results and excess of muons at sea level.

	Spectral index (β)	$A_p(\mathrm{cm^2\,s\,sr\,GeV})^{-1}$	Proton Intensity ($E_p > 10$ GeV) $(\mathrm{cm^2\,s\,sr})^{-1}$
Flare A	2.95 ± 0.47	3.4 ± 1.51	0.02 ± 0.011
Flare B[a]	3.1 ± 1.36	8.1 ± 3.51	0.031 ± 0.021

[a]Only the first peak

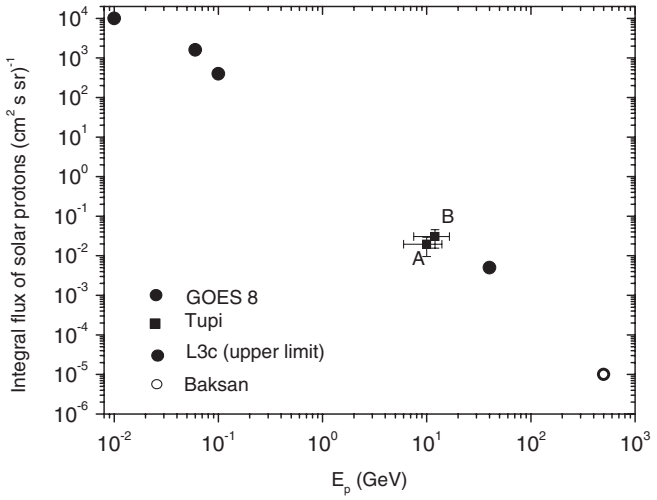

FIG. 12. The solar flare induced proton flux (Integral energy spectrum) obtained by this work (A and B black squares) and compared with other measurements [18].

it can be tied to a scale-free power-law energy spectrum of particles accelerated by solar flares. The similarity exists even when compared to solar flares of large scale. Some distortions can be related to the uncertainty in the determination of the spectral index, as shown in Fig. 12 of the integral energy spectrum, and a comparison with other measurements, such as the GOES 8 proton flux, the L3 Collaboration results, both for the flare on 14 July 2000, and the Baksan proton flux for the flare on 29 September 1989 (Ref. [18] and references therein).

IX. CONCLUSIONS

Solar flares release energy in many forms, from electromagnetic waves (gamma-rays and x-rays), to charged particles (protons, ions and electrons), and mass flows. Flares are characterized by their brightness in x-ray flux. In most cases, only flares of X-class and M-class (flux above 10^{-4} and 10^{-5} Watt m^2 respectively) are observed by ground detectors. However, we report here two C-class flares observed as muon excesses by the vertical Tupi telescope located at sea level and within the SAA region, where the shielding effect of the magnetosphere has a ''dip'' due to the anomalously weak geomagnetic field strength.

We have shown that both events of muon excess ($E_\mu > 100$ GeV) are in excellent correlation with solar flares whose x-ray prompt emissions have been reported by GOES 14, as well as in excellent correlation with the gamma-ray emissions observed by Fermi GBM. In addition, from an analysis on the basis of Monte Carlo results for the proton muon conversion in the atmosphere, and the rise time in muon time profiles, and their pitch angles, we conclude that the second event on 3 November 2010 is constituted at least by two extremely coherent muon pulses. This means that the particles, producing muons in the Earth's atmosphere, were emitted by the Sun, and their transport to Earth was practically nondiffuse. As for the first event, registered on 4 October 2010, the transport conditions between the Sun and the Earth were not very favorable. Nevertheless, it has a good correlation with both the GOES 14 x-ray flux and the Fermi GBM gamma-ray counting rate.

The energy spectra of accelerated protons evolve from soft to hard, with a gradual hardening with time. The transition from soft to hard can be due to energy loss of particles via nuclear collision (pion production) mechanisms, because it happens close to the energy threshold of pion production. In other words, there is the possibility of a scale-free energy distribution of particles accelerated by solar flares. Large and small scale flares have the same power-law energy spectrum, up to energies exceeding the pion production. If this hypothesis is correct, the vertical telescope is registering muons produced by protons (ions) whose energy corresponds to the high energy tail of the small scale flare spectrum. Consequently, the energy distribution of the emitted protons has to be a power-law spectrum, since power-law distributions are characterized as scale-free distributions.

ACKNOWLEDGMENTS

This work is supported by the National Council for Research (CNPq) of Brazil, under Grant No. 479813/2004-3 and Grant No. 476498/2007-4. We wish to express our thanks to Dr. Dennis Brian from RHESSI Mission for supplying data on the solar flares observed by Fermi. We are also grateful to various catalogs available on web and to their open data policy, especially to The ACE Science Center and the Fermi GBM Catalog.

[1] L. Svalgaard and H. Hudson, RHESSI Science Nugget: Cycle 24 - Don't Panic Yet!, http://sprg.ssl.berkeley.edu/~tohban/wiki/index.php/Cycle_24_-_don't_panic_yet!.
[2] P. Meyer, E. N. Parker, and J. A. Simpson, Phys. Rev. **104**, 768 (1956).
[3] J. A. Simpson, Space Sci. Rev. **93**, 11 (2000).
[4] H. Moraal, A. Belov, and J. M. Clem, Space Sci. Rev. **93**, 285 (2000).
[5] C. E. Navia, C. R. A. Augusto, M. B. Robba, M. Malheiro, and H. Shigueoka, Astrophys. J. **621**, 1137 (2005).
[6] C. R. A. Augusto, C. E. Navia, and M. B. Robba, Phys. Rev. D **71**, 103011 (2005).

[7] C. R. A. Augusto, C. E. Navia, and K. H. Tsui, Phys. Rev. D **77**, 123008 (2008).
[8] C. E. Barton, J. Geomagn. Geoelectr. **49**, 123 (1997).
[9] M. A. Abdu, I. S. Batista, A. J. Carrasco, and C. G. M. Brum, J. Atmos. Sol. Terr. Phys. **67**, 1643 (2005).
[10] C. R. A. Augusto *et al.*, Astropart. Phys.**34**, 40 (2010).
[11] S. K. Mitra, Nature (London) **142**, 914 (1938).
[12] S. P. Gupta, Adv. Space Res. **34**, 1798 (2004).
[13] D. Ruffolo and T. Khumlumlert, in *24th International Cosmic Ray Conference, Rome, 1995*, edited by N. Iucci and E. Lamanna (International Union of Pure and Applied Physics, London, 1995), p. 227.
[14] M. Honda *et al.*, Phys. Rev. D **70**, 043008 (2004).
[15] J. Poirier and C. D'Andrea, J. Geophys. Res. **107**, 1376 (2002).
[16] R. A. Mewaldt *et al.*, in *29th International Cosmic Ray Conference, Prune, India, 2005*, edited by B. Sripathi Acharya *et al.* (Tata Institute of Fundamental Research, Mumbai, 2005), p. 111.
[17] D. F. Smart and M. A. Shea, *21st International Cosmic Ray Conference, Adelaide, Australia, 1990*, edited by R. J. Protheroe (International Union of Pure and Applied Physics, London, 1990), p. 257.
[18] P. Achard *et al.*, Astron. Astrophys. **456**, 351 (2006).
[19] M. I. Dulding, PASA **18**, 12 (1994).